NACA RM E58B27

NACA

RESEARCH MEMORANDUM

INVESTIGATION OF A 0.6 HUB-TIP RADIUS-RATIO TRANSONIC TURBINE DESIGNED FOR SECONDARY-FLOW STUDY IV - ROTOR LOSS PATTERNS AS DETERMINED BY HOT-WIRE ANEMOMETERS WITH ROTOR OPERATING IN A CIRCUMFERENTIALLY UNIFORM INLET FLOW FIELD

By Milton G. Kofskey and Hubert W. Allen

Lewis Flight Propulsion Laboratory
Cleveland, Ohio

Declassified April 23, 1962

NATIONAL ADVISORY COMMITTEE FOR AERONAUTICS

WASHINGTON

May 20, 1958

NACA RM E58B27

NATIONAL ADVISORY COMMITTEE FOR AERONAUTICS

RESEARCH MEMORANDUM

INVESTIGATION OF A 0.6 HUB-TIP RADIUS-RATIO TRANSONIC TURBINE DESIGNED FOR SECONDARY-FLOW STUDY

IV - ROTOR LOSS PATTERNS AS DETERMINED BY HOT-WIRE ANEMOMETERS WITH ROTOR OPERATING IN A CIRCUMFERENTIALLY UNIFORM INLET FLOW FIELD

By Milton G. Kofskey and Hubert W. Allen

4830 CR-1

SUMMARY

Circumferential traces of specific-mass-flow variation for various radial positions at the rotor exit were obtained by the use of hot-wire anemometers. The comparatively uniform flow field at the rotor inlet gave suitable conditions for studying the secondary-flow behavior through a rotor blade row with minimized induced effects of secondary flow and wake losses generated by an upstream stator blade row. By supplementing the traces of specific-mass-flow variations with data obtained by time-averaging instruments, the specific-mass-flow data were converted to values of relative total-pressure ratio across the turbine rotor.

The combination of low loss near the hub and a high-loss region along the suction side of the blade wake at approximately 25 percent of the blade height indicated that low-momentum fluid along the hub accumulated along the suction side of the blade because of cross-channel flow and was then centrifuged toward the tip. Since the rotor blade was designed for high pressure-surface diffusion near the leading edge where the radially inward pressure force is greater than the centrifugal force, low-momentum fluid resulting from high diffusion flowed toward the hub in the thickened pressure surface boundary layer and contributed to the low-momentum fluid in the hub boundary layer. The increase in loss with increasing radial height from approximately 60 to 95 percent of the blade height indicated that the low-momentum fluid in the outer-wall boundary layer was being "scraped up" by the rotor blade tip.

Results of surveys taken at axial stations 0.188 and 3.2 inches downstream of the rotor trailing edge indicated that low-momentum fluid originating along the hub in the rotor passage was centrifuged toward the outer wall as it moved downstream.

INTRODUCTION

As part of the basic program of determining the sources and significance of losses within turbomachines, considerable information has been obtained on secondary-flow behavior through turbine stator rows at high and low air velocities (refs. 1 to 3).

The study of secondary-flow behavior in turbine rotor passages, however, has been accomplished chiefly by smoke flow investigations at low air and wheel speeds (refs. 3 and 4). The investigation of rotor secondary-flow phenomena at high air velocities, based on rotor-exit surveys of total pressure, total temperature, and angle such as reported in reference 5, has been complicated by two major factors. First, it is exceedingly difficult to separate upstream stator blade secondary flows and wake losses (as well as their effects) from losses generated by the rotor blade row. Second, low-frequency-response instruments used in taking surveys downstream of rotating blade rows complicate the problem of interpreting the results in view of the complex flow behavior.

In the present investigation of the secondary-flow behavior in rotating blade rows at high air and blade speeds, the problems associated with upstream stator loss accumulations and high air and blade speeds were greatly simplified by using a semivaneless stator configuration and hot-wire anemometers having high frequency response. Results of detailed surveys (ref. 6) taken downstream of the semivaneless stator configuration indicated that stator-exit loss accumulations had been effectively eliminated and therefore gave a flow field at the rotor inlet that was suitable for determining the pattern of losses originating in the rotor passage.

The study of the flow phenomena in the rotor passage boundary layers requires a knowledge of the instantaneous flow pattern at the rotor discharge. These measurements, as has been stated, are beyond the range of conventional measuring instruments because of the limitations of frequency response. Therefore, hot-wire anemometers with high frequency response are an ideal type of instrument for obtaining measurements of the instantaneous flow patterns at the rotor discharge.

With the attainment of a comparatively uniform flow field at the rotor inlet and with hot-wire traces of the instantaneous flow variation across the rotor passage for various radial positions, information concerning the flow phenomena in the rotor passage boundary layers was obtained. The flow characteristics through the rotor passage are described herein, and factors that influence the indicated flow patterns are discussed.

4830

SYMBOLS

c_p	specific heat at constant pressure, Btu/(lb)($^{\circ}$R)
$\bar{e}_w$	average value of wire voltage, volts
Δe_w	difference between instantaneous wire voltage (obtained from trace) and average value of wire voltage, volts
e_o	value of wire voltage at zero flow, volts
g	acceleration due to gravity, 32.2 ft/sec^2
J	mechanical equivalent of heat, 778.2 ft-lb/Btu
P	total pressure, lb/sq ft
T	total temperature, $^{\circ}$R
t	static temperature, $^{\circ}$R
U	blade velocity, ft/sec
V	absolute velocity, ft/sec
$\bar{V}$	absolute velocity obtained from measurements by time-averaging probes, ft/sec
W	relative velocity, ft/sec
$\bar{W}$	relative velocity obtained from measurements by time-averaging probes, ft/sec
$\bar{\alpha}$	absolute discharge angle as measured from axial direction by time-averaging probes, deg
$\bar{\beta}$	relative discharge angle as measured from axial direction, deg
γ	ratio of specific heats
η	local efficiency based on measured values of inlet and outlet total state
ρ	density, lb/cu ft
$\overline{\rho V}$	time-average value of mass flow obtained from surveys of total pressure, temperature, and wall static pressure, lb/(sq ft)(sec)

$\Delta(\rho V)$ difference between $\overline{\rho V}$ and instantaneous ρV, lb/(sq ft)(sec)

ν flow angle of instantaneous velocity measured from tangential direction, deg

φ flow angle of instantaneous relative velocity measured from tangential direction, deg

Subscripts:

cr conditions at Mach number of 1.0

θ tangential direction

1 upstream of rotor

2 downstream of rotor

Superscript:

" relative to rotor

4830

APPARATUS AND INSTRUMENTATION

The components of the cold-air test facility, described in reference 6, consisted primarily of inlet piping for combustion air supply, filter and inlet tanks, turbine test section, discharge collector and piping, and an eddy current dynamometer. The design and performance of the semivaneless stator with a transonic rotor is described in detail in references 6 and 7.

The instrumentation and method of turbine operation were the same as described in reference 8, except that an additional survey station was located approximately 0.188 inch downstream of the rotor trailing edge and the pressure, angle, and temperature surveys were supplemented by a radial survey of specific mass flow with hot-wire anemometers. The total pressure, angle, and total temperature were surveyed with a combination probe that was operated with a pressure transducer and X-Y recorders.

The hot-wire-anemometer probe used a 0.0002-inch-diameter tungsten wire with an effective length of 0.080 inch. The axis of the wire was parallel to the axis of the probe and therefore the hot-wire anemometer was sensitive to the circumferential and axial velocities. A sketch of the probe is shown in figure 1(a). The hot-wire anemometer was of the constant-temperature type discussed in reference 9 and had a maximum frequency response of at least 40,000 cycles per second. Therefore, with the small physical dimensions of the wire and the high frequency response of the system, the clear definition of the rotor blade wake was possible.

A block diagram of the hot-wire circuit is shown in figure 1(b). The hot wire forms one arm of a bridge in which balance is maintained by an amplifier as discussed in reference 9. The bridge voltage variations are observed on the Y-axis of the oscilloscope. The sweep frequency was synchronized to the rotor frequency by means of a magnetic pickup located on the dynamometer housing near the rotor shaft.

REDUCTION OF HOT-WIRE DATA

4830

The instantaneous value of ρV is calculated from hot-wire data by use of the following equation, which is derived in reference 9:

$$\frac{\Delta(\rho V)}{\overline{\rho V}} = \frac{4\Delta\bar{e}_w}{\bar{e}_w^2 - e_0^2}\Delta e_w$$

By solving for $\Delta(\rho V)/\overline{\rho V}$ and using values of ρ and $\overline{\rho V}$ from surveys of total pressure, total temperature, and wall static pressure and by neglecting the radial component, the instantaneous value of absolute velocity V is obtained. The static pressure may be assumed constant circumferentially across the rotor blade wake at any given radius, but the static temperature in the wake will be between the free-stream value and the total temperature because of turbulence. Therefore, the density may be slightly different in the wake from that in the free stream. However, the difference between the temperature in the wake and in the free stream will be so small that the variations in density across the rotor exit will be negligible.

In order to calculate the relative velocity W the relative discharge angle across the rotor blade wake at a given radius is assumed constant. The relative discharge angle $\bar{\beta}$ is obtained from the results of the survey and the rotor speed U. A velocity diagram is shown in figure 2. Since the relative discharge angle and the rotor speed will remain constant circumferentially at a given radius, the relative velocity can be obtained from the absolute velocity obtained from hot-wire data and the following equation:

$$W = \frac{V \sin \nu}{\sin \varphi} \tag{1}$$

Once the relative and absolute velocities and total temperature are known, the relative total-pressure ratio P_2''/P_1'' can be calculated. Since

$$\frac{P_2''}{P_2} = \left(\frac{T_2''}{T_2}\right)^{\frac{\gamma}{\gamma-1}} \tag{2}$$

and

$$T_2'' = t_2 + \frac{W_2^2}{2gJc_p}$$

$$t_2 = T_2 - \frac{V_2^2}{2gJc_p}$$

therefore

$$\frac{T_2''}{T_2} = 1 - \frac{V_2^2 - W_2^2}{2gJc_pT_2} \tag{3}$$

Substituting equation (3) into equation (2) yields

$$P_2'' = P_2\left(1 - \frac{V_2^2 - W_2^2}{2gJc_pT_2}\right)^{\frac{\gamma}{\gamma-1}} \tag{4}$$

At the rotor inlet

$$\frac{T_1''}{T_1} = 1 - \frac{\gamma - 1}{\gamma + 1}\frac{U}{V_{cr,1}}\left[2\left(\frac{V_\theta}{V_{cr}}\right)_1 - \frac{U}{V_{cr,1}}\right] \tag{5}$$

and

$$\frac{P_1''}{P_1} = \left(\frac{T_1''}{T_1}\right)^{\frac{\gamma}{\gamma-1}} \tag{6}$$

Therefore, substitution of equation (5) into equation (6) yields

$$P_1'' = P_1\left\{1 - \frac{\gamma - 1}{\gamma + 1}\frac{U}{V_{cr,1}}\left[2\left(\frac{V_\theta}{V_{cr}}\right)_1 - \frac{U}{V_{cr,1}}\right]\right\}^{\frac{\gamma}{\gamma-1}} \tag{7}$$

Equations (4) and (7) are expressed in the desired total-pressure ratio across the rotor as follows:

4830

$$\frac{P_2''}{P_1''} = \frac{P_2}{P_1}\left(\frac{1 - \dfrac{V_2^2 - W_2^2}{2gJc_pT_2}}{1 - \dfrac{\gamma - 1}{\gamma + 1}\dfrac{U}{V_{cr,1}}\left[2\left(\dfrac{V_\theta}{V_{cr}}\right)_1 - \dfrac{U}{V_{cr,1}}\right]}\right)^{\frac{\gamma}{\gamma-1}} \tag{8}$$

The values of P_1, $U/V_{cr,1}$, and $(V_\theta/V_{cr})_1$ were obtained from previous surveys taken at design conditions.

4830

Since there was negligible circumferential variation of rotor inlet total pressure at a given radius, it was possible to use an average radial distribution of inlet total pressure as a basis for determining relative total-pressure-loss distribution in the rotor passages. Since measured values were used at the rotor inlet, the values of relative pressure ratio are a good indication of rotor blade performance.

RESULTS AND DISCUSSION

Rotor Blade-Wake Traces

Specific-mass-flow traces taken with a radial hot wire located approximately 0.188 inch downstream of the rotor blade trailing edge are presented in figure 3. Traces are shown from approximately 5 to 95 percent of the blade height. As the trace on the oscilloscope screen moves from left to right across the screen, any losses along the suction surface of the blade appear on the left side of the wake of the trace (fig. 3(c)).

Inspection of the specific-mass-flow traces of figure 3 shows that well-defined rotor blade wakes are obtained from approximately 20 to 90 percent of the blade height. From approximately 5 to 10 percent of the blade height, the traces show little variation. At 20 to approximately 40 percent and 80 to 90 percent of blade height, there is a mass-flow deficiency along the suction side of the blade. From 40 to 60 percent of the blade height, a deficiency appears on the pressure side of the blade. Observation of numerous photographs of hot-wire traces taken with a 16-millimeter movie camera as the hot-wire probe was moved radially from 90 to 95 percent of the blade height revealed that the loss region that developed adjacent to the wake increased in magnitude with increasing radial height. At a radial height of 95 percent, this loss region was greater in magnitude than the loss in the blade wake.

Relative Total-Pressure Ratio

Figure 4 presents a contour plot of relative total-pressure ratio across the rotor. As was explained previously, the loss distribution in relative total pressure at the rotor exit is primarily produced in the rotor itself.

A low-loss region is shown from 5 to approximately 15 percent of the blade height. At approximately 25 percent, there is a region of low-momentum fluid or high loss along the suction side of the rotor blade. The low-loss region at approximately 5 to 15 percent of the blade height and the region of high loss along the suction side of the blade at approximately 25 percent of blade height can be explained in the following manner. With relative conditions, low-momentum fluid in the hub boundary layer flows cross channel from the pressure surface of one blade to the suction surface of the adjacent rotor blade because of the cross-channel pressure gradient and rolls up against the suction surface of the blade. Since the outward centrifugal forces are greater than the inward radial pressure forces near the trailing portion of the blade, the region of low-momentum fluid is centrifuged outward. Photographs of smoke flow traces of cross-channel flow through stator blade rows are presented in reference 1. With relative conditions for the rotor blade case, cross-channel flow along the hub of a rotor blade row will therefore be similar to that found along the inner wall of a stator blade row.

As was explained in reference 8, the rotor blade was designed for relatively high pressure-surface diffusion near the leading edge. This design can result in thickening of the pressure-surface boundary layer with possible flow separation. Thus, low-momentum fluid resulting from the high diffusion could flow toward the hub in the thickened boundary layer and contribute to the low-momentum fluid in the hub boundary layer, since the radial pressure force associated with the high amount of whirl near the leading edge would predominate over centrifugal forces. A schematic diagram of the secondary-flow components is presented in figure 5. Reference 5, which compares two turbine configurations, one having high rotor blade suction-surface diffusion near the trailing edge and the other having high pressure-surface diffusion near the leading edge, shows that the location and surface having high diffusion affected the loss pattern at the rotor discharge. The loss pattern obtained for the configuration having high pressure-surface diffusion near the leading edge indicated loss patterns similar to those obtained with the subject turbine.

As shown in figure 3 and the contours of relative total-pressure ratio of figure 4, there may be a bleedoff of low-momentum fluid from the pressure side of the rotor blade at a radial height of approximately 40 to 60 percent of the blade height. This region of low-momentum fluid may be part of thickened boundary layer bleeding off the pressure surface. A schematic diagram of this phenomenon is shown in figure 6.

4830

The accumulation of low-momentum fluid along the suction side of the rotor blade increases in size and magnitude of loss with increasing radial height from approximately 60 to 95 percent of blade height (figs. 3 and 4). This accumulation of low-momentum fluid along the suction surface of the blade is probably the result of the scraping up of the outer-wall boundary layer by the rotor blade. Smoke flow investigations of this secondary-flow phenomenon at the rotor blade tip are reported in references 3 and 4. As stated in reference 4, secondary flows that appear in the rotor tip region include the cross-channel flow in the outer-wall boundary layer and the passage vortex that appears in some stationary shrouded blade rows. However, the tip-clearance space and the relative motion between rotor blade tip and outer wall result in additional flows and modifications of the cross-channel flow. Cross-channel flow is increased by the addition of the relative velocity component toward the suction surface due to the rotor blade tip speed. Since the ratio of rotor tip speed to axial air velocity is greater than 0.8 and the angle of incidence is approximately 0°, it appears from figure 13 of reference 4 that, for the subject turbine, a scraping vortex would be formed along the suction surface near the rotor blade tip. The interaction of any centrifuging of low-momentum fluid along the blade suction surface and blade wake with the scraping vortex is shown schematically in figure 7.

Figure 4 shows a region of relative total-pressure ratio greater than 1.00 at approximately 95 percent of the blade height and near the pressure side of the wake. Relative total-pressure ratio at any radial height at the rotor outlet is based on the value of the relative total pressure at the corresponding radial height at the rotor inlet. Values of relative total-pressure ratio greater than 1.00 can be obtained for a condition in which a fluid particle, at the free-stream value of total pressure and adjacent to the outer-wall boundary layer, shifts radially outward in passing through the blade passage. Upon reaching the rotor exit, the fluid particle is at a radial height corresponding to a position in the wall boundary layer at the rotor inlet where the total pressure is less than the free-stream value.

The region of relative total-pressure ratios greater than 1.00 (fig. 4) results from the accumulation of the thick outer-wall boundary along the suction side of the blade wake. Fluid at or near the free-stream value of relative total pressure at the rotor inlet shifts radially toward the outer wall when passing through the rotor passage to fill this region (along pressure side of blade wake) where the boundary-layer thickness is reduced.

Centrifuging of Low-Momentum Fluid

Figure 8 presents a plot of local efficiency against blade height for surveys taken at axial locations approximately 0.188 and 3.2 inches

(ref. 5) or 1 chord length downstream of the rotor trailing edge. The survey station located nearer the blade trailing edge shows the region of low local efficiency (resulting from the rollup of the boundary layer from the rotor hub) occurring at approximately 30 percent of the blade height. This region of low local efficiency apparently is centrifuged outward as it moves downstream and appears at approximately 60 percent of the blade height at the measuring station 1 chord length downstream of the rotor blade trailing edge. A schematic diagram of the path of the core of low-momentum fluid being centrifuged outward is shown in figure 9.

From these results, it is apparent that caution should be exercised in determining origins of low efficiencies when the survey station is located sufficiently downstream and centrifuging of low-momentum fluid can materially change the position of low efficiency.

CONCLUDING REMARKS

The semivaneless stator configuration used in the investigation effectively eliminated stator-exit loss accumulations and therefore gave a uniform flow field at the rotor inlet. The combination of a uniform flow field at the rotor inlet and the use of hot-wire anemometers, which measured circumferential time variation of specific mass flow at the rotor exit, gave suitable conditions for obtaining information on the secondary flows through a rotor blade row with minimized induced effects produced by secondary flow and wake losses of an upstream stator blade row.

From approximately 5 to 10 percent of the blade height, little circumferential variation was observed in specific mass flow in the free stream and in the rotor blade wake.

Contours of relative total-pressure ratio across the rotor indicated that the hub boundary layer flowed cross channel from the blade pressure surface to the suction surface of the adjacent blade. Because the rotor blade was designed for high pressure-surface diffusion near the leading edge (where the inward radial pressure force is greater than the centrifugal force), low-momentum fluid resulting from the high diffusion moved toward the hub and contributed to the low-momentum fluid in the hub boundary layer. When the low-momentum fluid in the boundary layer reached the suction surface near the trailing edge, the low-momentum fluid was centrifuged toward the tip, since the centrifugal force was greater than the radial pressure force.

The accumulation of low-momentum fluid along the suction surface of the blade increased in size and magnitude of loss with increasing radial height from approximately 60 to 95 percent of the blade height. This accumulation of low-momentum fluid is probably the result of the scraping up of the outer-wall boundary layer by the rotor blade tip.

Surveys taken at approximately 0.188 and 3.2 inches downstream of the rotor blade indicated that the region of low-momentum fluid near the hub was centrifuged toward the tip as it moved downstream.

Lewis Flight Propulsion Laboratory
National Advisory Committee for Aeronautics
Cleveland, Ohio, March 6, 1958

4830
CR-2 back

REFERENCES

1. Rohlik, Harold E., Kofskey, Milton G., Allen, Hubert W., and Herzig, Howard Z.: Secondary Flows and Boundary-Layer Accumulations in Turbine Nozzles. NACA Rep. 1168, 1954. (Supersedes NACA TN's 2871, 2909, and 2989.)

2. Herzig, Howard Z., Hansen, Arthur G., and Costello, George R.: A Visualization Study of Secondary Flows in Cascades. NACA Rep. 1163, 1954. (Supersedes NACA TN 2947.)

3. Kofskey, Milton G., and Allen, Hubert W.: Smoke Study of Nozzle Secondary Flows in a Low-Speed Turbine. NACA TN 3260, 1954.

4. Allen, Hubert W., and Kofskey, Milton G.: Visualization Study of Secondary Flows in Turbine Rotor Tip Regions. NACA TN 3519, 1955.

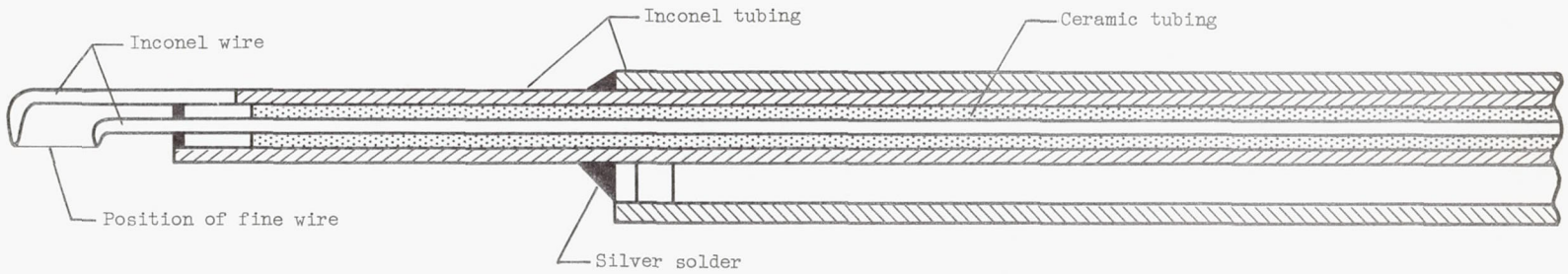
5. Wong, Robert Y., Miser, James W., and Stewart, Warner L.: Qualitative Study of Flow Characteristics Through Single-Stage Turbines as Made from Rotor-Exit Surveys. NACA RM E55K21, 1956.

6. Rohlik, Harold E., and Wintucky, William T.: Investigation of a Semivaneless Turbine Stator Designed to Produce Axially Symmetrical Free-Vortex Flow. NACA TN 3980, 1957.

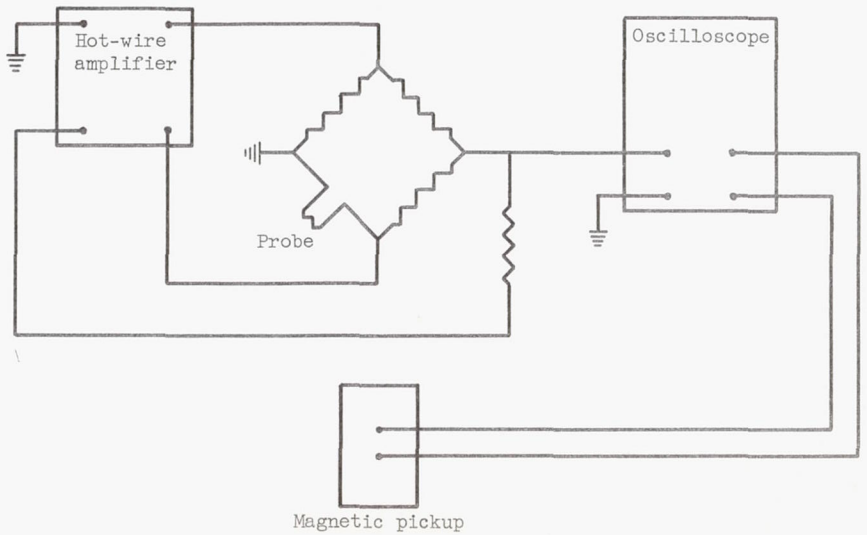
7. Rohlik, Harold E., Wintucky, William T., and Moffitt, Thomas P.: Investigation of a 0.6 Hub-Tip Radius-Ratio Transonic Turbine Designed for Secondary-Flow Study. III - Experimental Performance with Two Stator Configurations Designed to Eliminate Blade Wakes and Secondary-Flow Effects and Conclusions from Entire Stator Investigation. NACA RM E57G08, 1957.

8. Rohlik, Harold E., Wintucky, William T., and Scibbe, Herbert W.: Investigation of a 0.6 Hub-Tip Radius-Ratio Transonic Turbine Designed for Secondary-Flow Study. I - Design and Experimental Performance of Standard Turbine. NACA RM E56J16, 1957.

9. Laurence, James C., and Landes, L. Gene.: Auxiliary Equipment and Techniques for Adapting the Constant-Temperature Hot-Wire Anemometer to Specific Problems in Air-Flow Measurements. NACA TN 2843, 1952.



(a) Hot-wire-anemometer probe.



(b) Block circuit diagram.

CD-6055

Figure 1. - Constant-temperature hot-wire anemometer.

4830

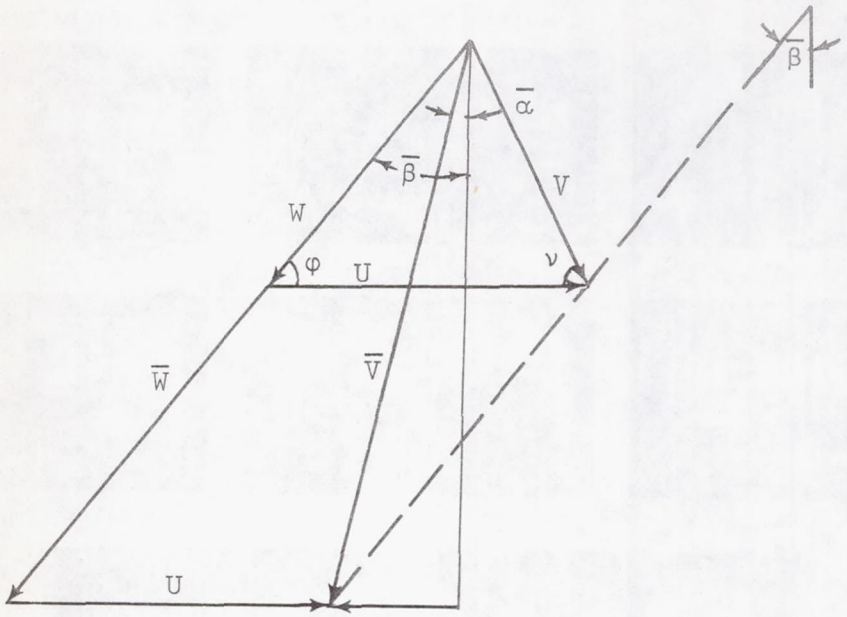
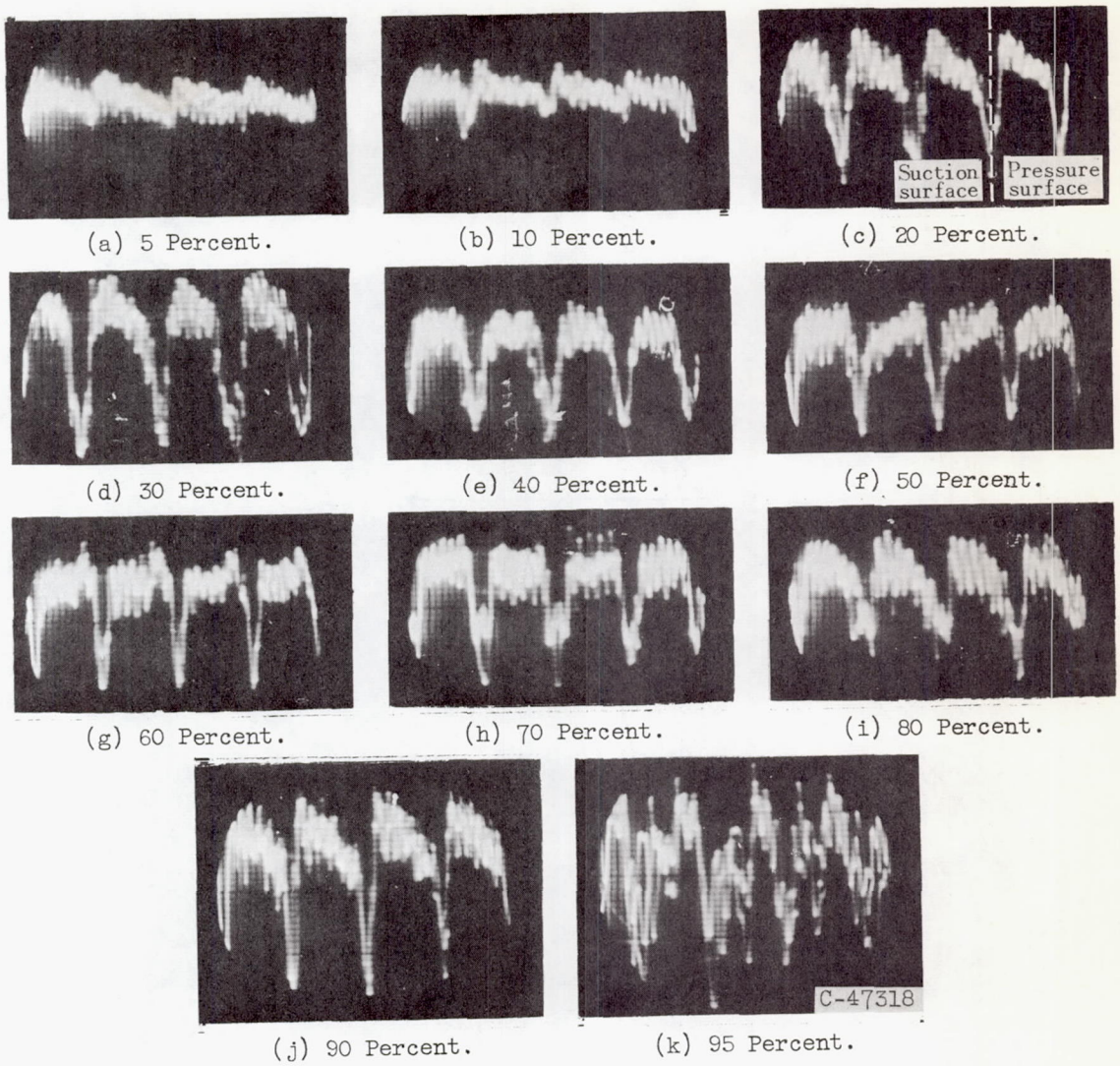


Figure 2. - Velocity diagrams for determination of relative velocity W.



(a) 5 Percent. (b) 10 Percent. (c) 20 Percent.

(d) 30 Percent. (e) 40 Percent. (f) 50 Percent.

(g) 60 Percent. (h) 70 Percent. (i) 80 Percent.

(j) 90 Percent. (k) 95 Percent.

Figure 3. - Hot-wire traces of specific-mass-flow variation at rotor discharge for various percentages of blade height as measured from hub.

4830

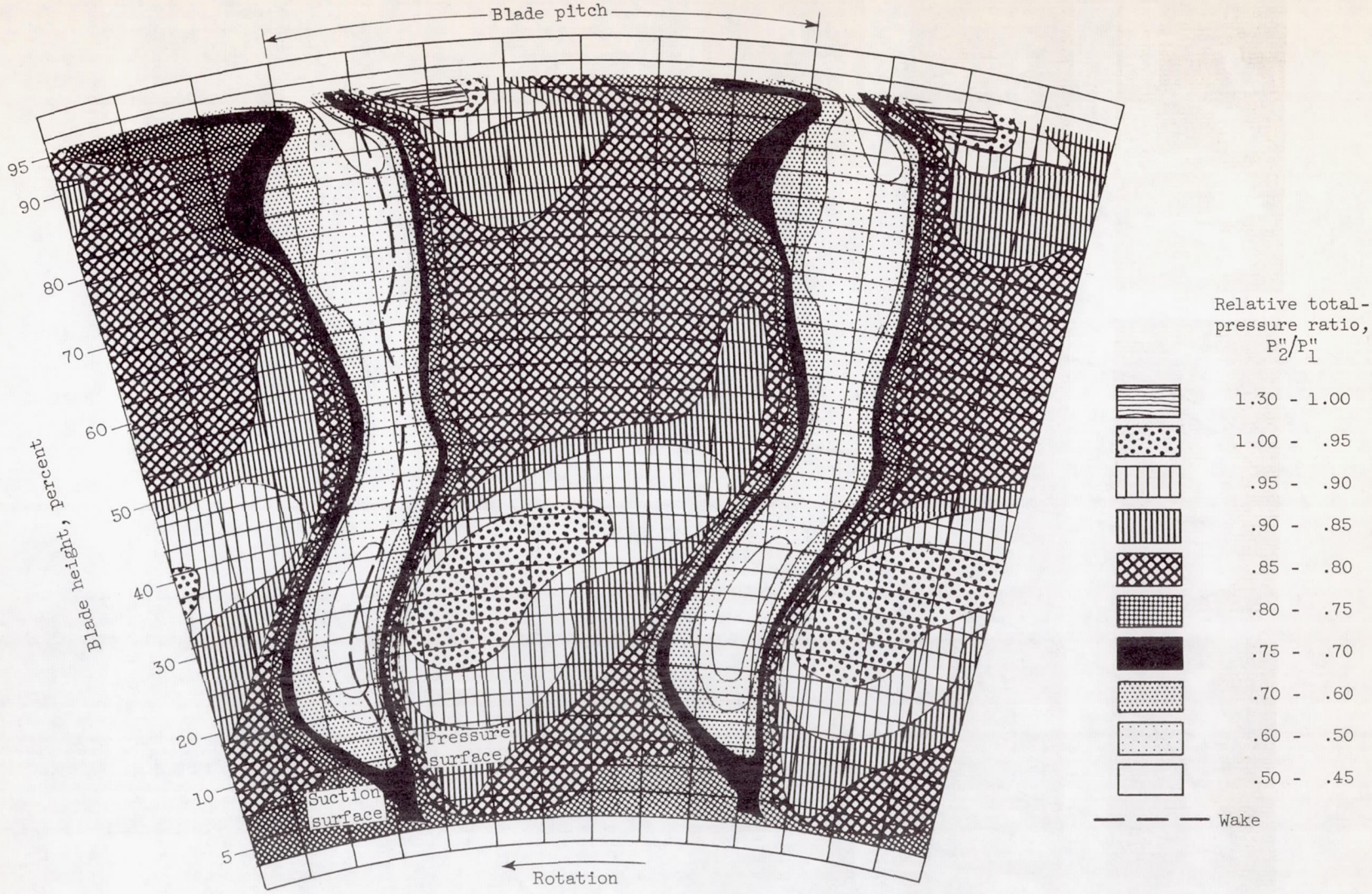


Figure 4. - Contours of relative total pressure ratio.

4830



Figure 5. - Flow path of blade losses from pressure-surface boundary layer and contribution to cross-channel flow at hub.

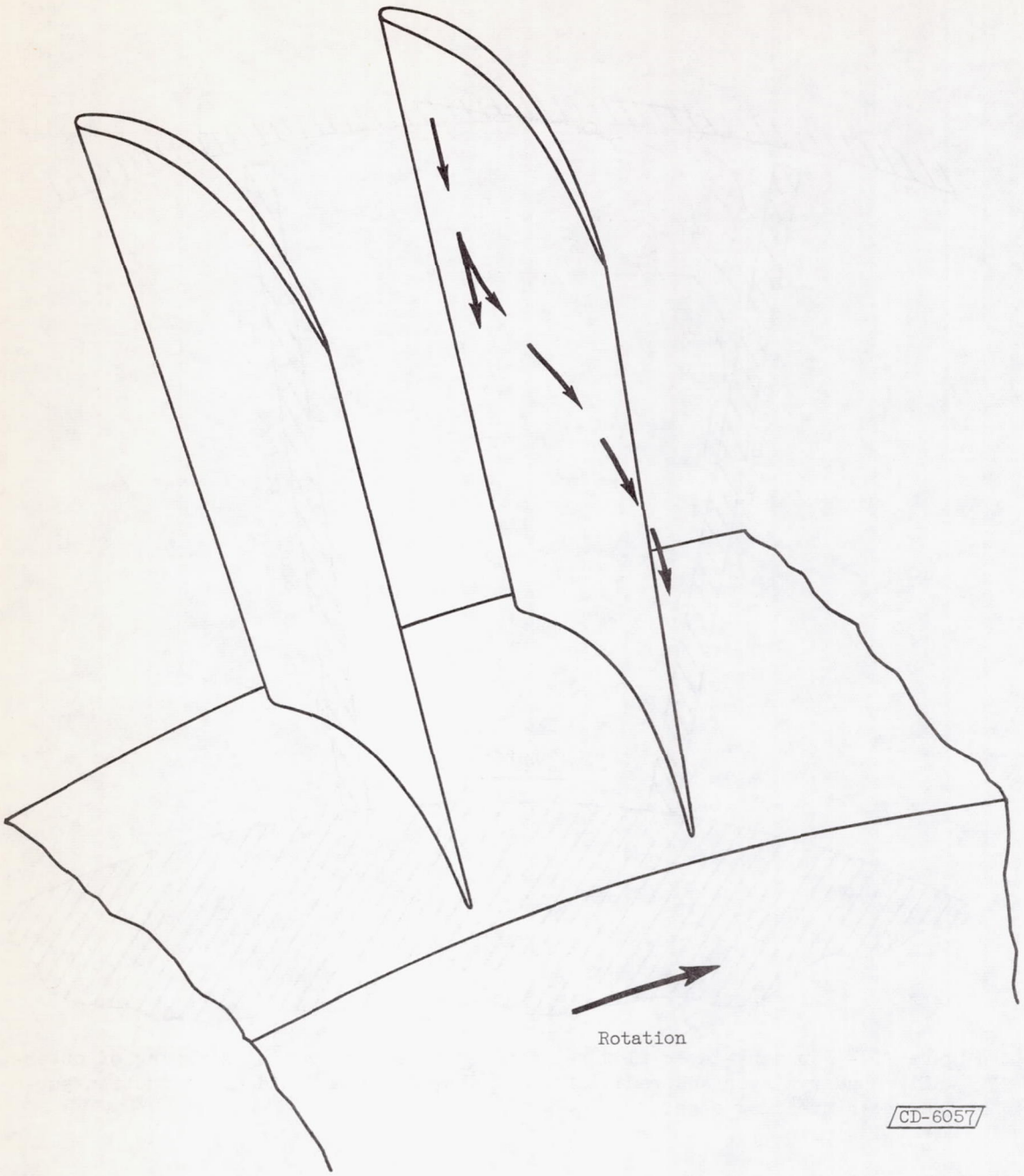


Figure 6. - Flow path in pressure-surface boundary layer.

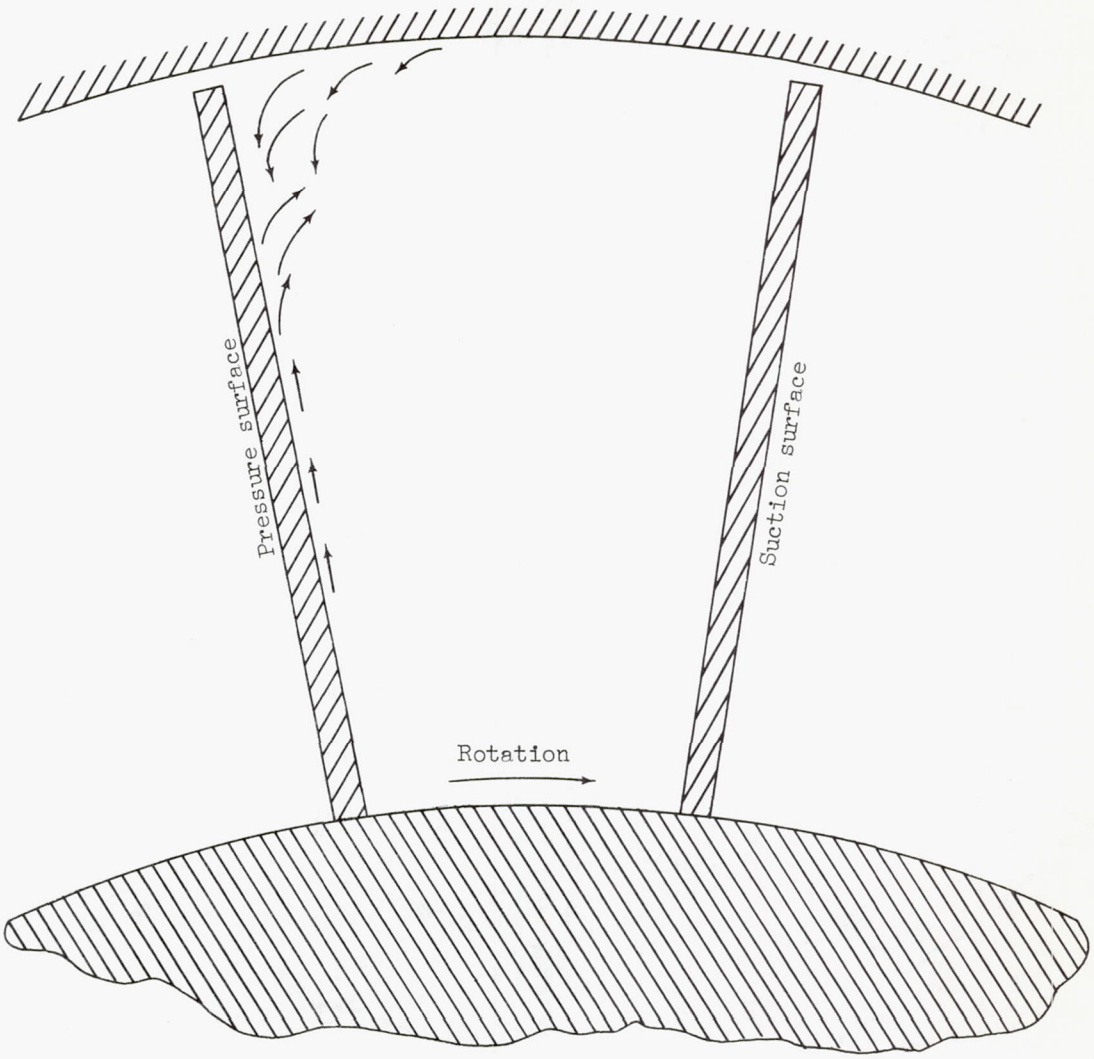


Figure 7. - Boundary-layer flow relative to blade indicating scraping of outer-wall boundary layer and radial flow of low-momentum fluid along suction surface near trailing edge.

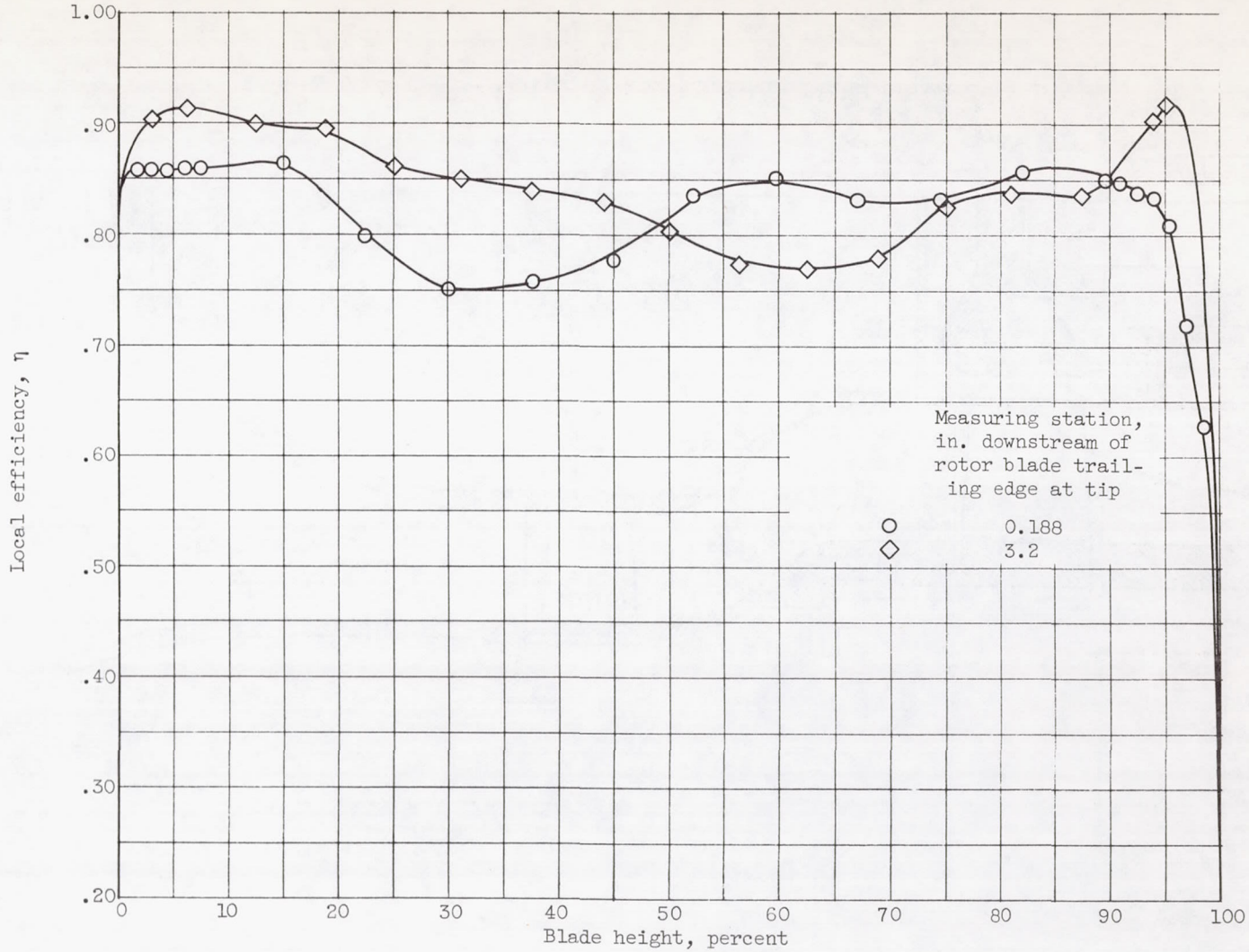


Figure 8. - Variation of local efficiency as determined by exit surveys.

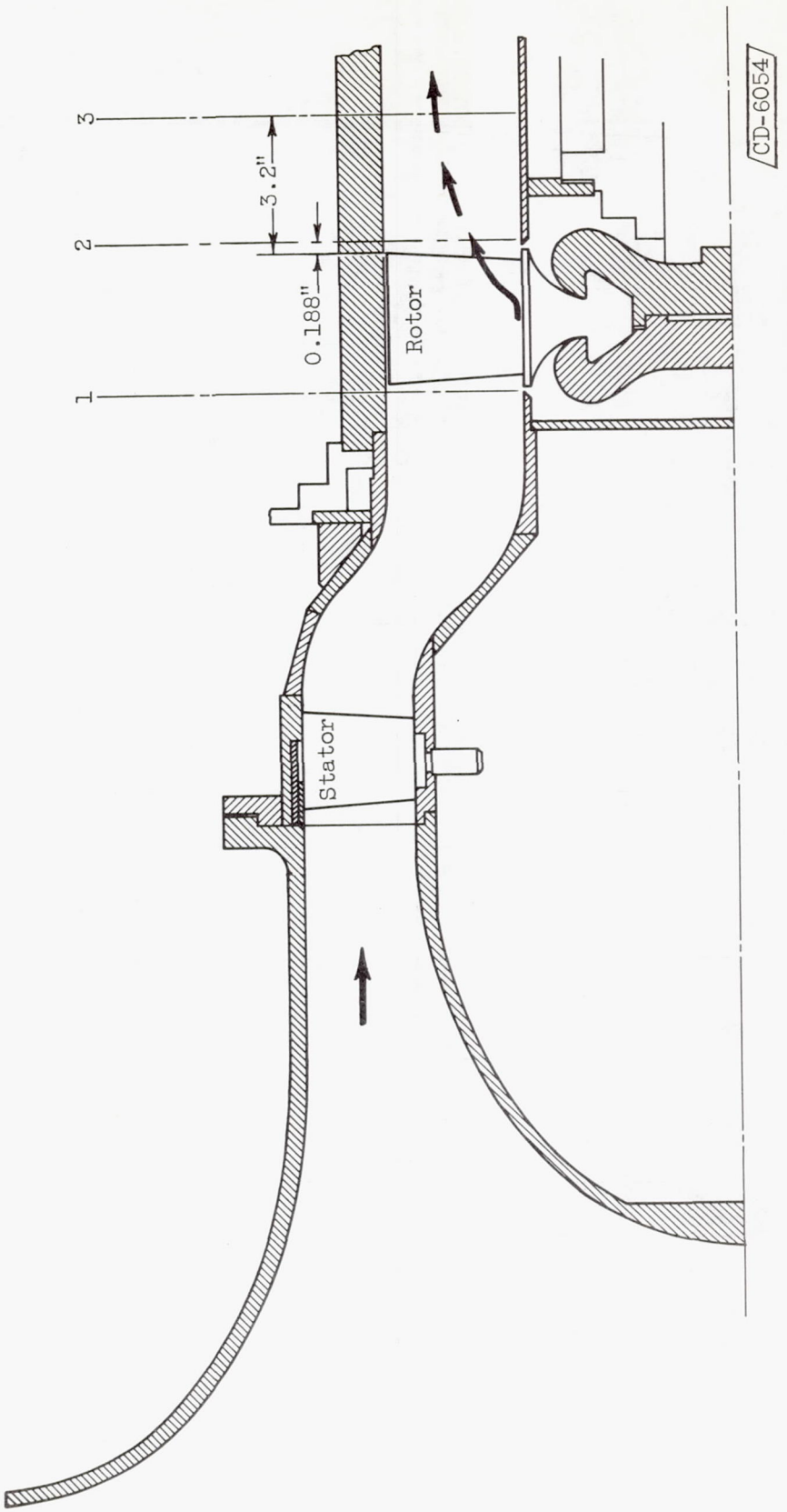


Figure 9. - Centrifuging of low-momentum fluid outward.